Precessing binary black holes as engines of electromagnetic helicity

Nicolas Sanchis-Gual[1,2] and Adrian del Rio[3]

[1]*Departament d'Astronomía i Astrofísica, Universitat de València, Dr. Moliner 50, 46100 Burjassot, València, Spain*

[2]*Departamento de Matemática, Universidade de Aveiro and Centre for Research and Development in Mathematics and Applications (CIDMA), Campus de Santiago, 3810-183 Aveiro, Portugal*

[3]*Departamento de Física Teórica and IFIC, Universitat de Valencia-CSIC, Dr. Moliner 50, 46100, Burjassot, Valencia, Spain*

(Received 3 April 2023; accepted 9 August 2023; published 24 August 2023)

We show that binary black hole mergers with precessing evolution can potentially excite photons from the quantum vacuum in such a way that total helicity is not preserved in the process. Helicity violation is allowed by quantum fluctuations that spoil the electric-magnetic duality symmetry of the classical Maxwell theory without charges. We show here that precessing binary black hole systems in astrophysics generate a flux of circularly polarized gravitational waves which, in turn, provides the required helical background that triggers this quantum effect. Solving the fully nonlinear Einstein's equations with numerical relativity we explore the parameter space of binary systems and extract the detailed dependence of the quantum effect with the spins of the two black holes. We also introduce a set of diagrammatic techniques that allows us to predict when a binary black hole merger can or cannot emit circularly polarized gravitational radiation, based on mirror-symmetry considerations. This framework allows to understand and to interpret correctly the numerical results, and to predict the outcomes in potentially interesting astrophysical systems.

DOI: 10.1103/PhysRevD.108.044052

I. INTRODUCTION

A dynamical spacetime can excite the quantum modes of the electromagnetic field and can produce as a result photons out of the quantum vacuum [1,2]. Well-known examples of this effect were explored long ago in cosmological backgrounds [3] and in the gravitational collapse of stars [4]. The particles created by the spacetime are entangled and in particular their physical properties respect the symmetries of the background. For instance, if the spacetime is spatially homogeneous, as is typical in cosmology, particles are produced in pairs and with opposite linear momentum. This is because of the invariance of the field modes or vacuum state under spatial translations. Similarly, the spherical symmetry of the Schwarzschild metric in a gravitational collapse requires that the Hawking pairs have opposite angular momentum. In other words, the symmetries of the background impose constraints on the particles created. If, on the other hand, the background spacetime does not possess these symmetries, then the particles created may not be subject to such limitations. To give an example, for the gravitational collapse of a rotating star, where spherical symmetry is lost, the spacetime dynamics can induce a net angular momentum in the flux of particles created, particle pairs are not necessarily created with opposite angular momenta [5].

In addition to the symmetries of the background, there are intrinsic symmetries of the quantum field that must be preserved during the process of particle creation. For instance, the electromagnetic theory must be gauge invariant, and if the electromagnetic field is coupled to fermion fields, this symmetry requires the conservation of the electric charge in any process. Interestingly, in some particular cases the background spacetime can induce fundamental violations of classical internal symmetries in the quantum theory. An example of this is the electric-magnetic duality symmetry of the source-free Maxwell theory. In the classical theory this symmetry guarantees that the circularly polarized state of electromagnetic waves remains constant during their propagation. Then, one could naively expect that, in any dynamical gravitational field, photons should be created in pairs of opposite helicity, so as to keep the same circular polarization state of the vacuum. However, it was found that this symmetry fails to survive the quantization in a gravitational field [6–9]. As a result, the net helicity need not be conserved, and photons are expected to be created without having to satisfy this constraint, provided the background spacetime is helical.

Given a fixed spacetime background that evolves between two asymptotically stationary configurations, a detailed study of how many photons are created in each helicity sector from this anomaly, as well as the frequency and angular spectrum, requires an explicit calculation of the Bogoliubov coefficients that relate "in" and "out" vacuum

states [1]. However, except for few well-known examples, this calculation is inaccessible with current theoretical techniques. Despite this, it is still possible to determine the average total amount of right-handed minus left-handed photons created. This quantity is accessible from the vacuum expectation value of the operator Q_5 that represents the classical Noether charge in the quantum theory. Indeed, the quantum anomaly indicates that the change in time of this expectation value is independent of the choice of quantum state and, furthermore, it only depends on the background geometry as

$$\Delta\hat{Q}_5 \equiv \langle\hat{Q}_5(t_2)\rangle - \langle\hat{Q}_5(t_1)\rangle = \frac{-\hbar}{96\pi^2}\int_{[t_1,t_2]\times\Sigma} d^4x\sqrt{-g}R_{abcd}{}^{*}R^{abcd}, \quad (1)$$

where $R^a{}_{bcd}$ denotes the Riemann tensor of the spacetime. The quotient $\Delta\hat{Q}_5/\hbar$ is the net average number difference between positive-helicity photons (or right-handed) and negative-helicity photons (or left-handed) created by the gravitational dynamics (integrated over all possible frequencies and momenta). Since this is fully determined by the spacetime geometry, it can be evaluated very easily with usual techniques in General Relativity. In compact manifolds without boundary the right-hand side of Eq. (1) is a topological invariant, called the Chern-Pontryagin scalar. In General Relativity and astrophysics, 4-dimensional spacetime manifolds of physical interest are neither compact nor boundaryless, and the Chern-Pontryagin does contain information about the geometry (i.e., about the gravitational field). Roughly speaking, it measures the helical nature of the spacetime. This is, the degree of gravitational chirality.

In a previous paper we proved that this quantum anomaly is produced whenever the spacetime background admits a flux of net circularly polarized gravitational radiation [10,11]. More precisely,

$$\langle\hat{Q}_5(\mathcal{J}^+)\rangle - \langle\hat{Q}_5(\mathcal{J}^-)\rangle = (...) + \hbar\int_0^\infty \frac{d\omega\omega^3}{24\pi^3}\sum_{\ell m}[|h_+^{\ell m}(\omega) - ih_\times^{\ell m}(\omega)|^2 - |h_+^{\ell m}(\omega) + ih_\times^{\ell m}(\omega)|^2], \quad (2)$$

where h_+, $h_\times$ denote the two linear polarization modes of gravitational waves that reach future null infinity, emitted by an arbitrary isolated gravitational source that is stationary at both past and future timelike infinities. These modes are characterized by the frequency ω, and angular momentum ℓ, m. The contribution denoted by dots corresponds to the flux of chiral gravitational flux falling through the black hole (BH) horizon. The explicit expression is tedious but will not be relevant in our discussion. The physical picture is simple; a nontrivial gravitational field can create a difference in the number of right- and left-handed circularly polarized photons from the quantum vacuum. The more right(left)-handed gravitational radiation is emitted by a system, the more right (left)-handed electromagnetic modes will be excited.

In this paper we examine in great detail which spacetime backgrounds in astrophysics can generate such gravitational wave flux. Using symmetry arguments and some diagrams we will be able to predict that precessing binary BH systems can potentially trigger this quantum effect. We will prove this rigorously solving the fully nonlinear Einstein's equations using standard techniques in numerical relativity, and explore the dependence with the relative masses and spins of the BHs. Notice on the other hand that the net difference of positive and negative photons (1) will be insensitive to the total mass of the system, since the integral on the rhs is adimensional and one can always rescale the coordinates by this mass.

Along this paper we work in geometric units $G = c = 1$. The present paper is a detailed exposition of the numerical results presented in [10], where the main results were communicated.

II. BINARY DIAGRAMS AND MIRROR SYMMETRY

Although it may seem a trivial question, it is actually difficult to find examples of physically interesting gravitational fields that make (1) nonzero. In fact, one can prove that all stationary, asymptotically flat solutions of Einstein's equations lead to a vanishing result [11]. As a consequence, one needs dynamical gravitational fields in the fully nonlinear regime, and, in turn, this requires the use of numerical relativity.

Unfortunately, solving Einstein's equations numerically is a computationally expensive task. To study this question efficiently, it is necessary first to have some guidance. If one restricts to binary BH systems in astrophysics, it is possible to infer which family of solutions can be expected to produce nontrivial results using just symmetry arguments. The key idea is to notice that (1) is a pseudoscalar. As a result, any binary system that is invariant under a mirror transformation with respect to, at least, one coordinate plane, will make this integral equal to zero. The goal then is to look for systems with no mirror symmetries.

Let us make this idea more precise. Consider a $3+1$ foliation of the spacetime manifold $M = I \times \Sigma$. In $3+1$ numerical relativity Einstein's equations are solved with 3-dimensional euclidean grids, so we will restrict to spatial slices with trivial topology, $\Sigma \simeq \mathbb{R}^3$[1] The different binary BH systems are uniquely represented by a 4-dimensional

[1]For spacetimes involving black holes a convenient $3+1$ foliation is engineered to bypass the curvature singularities, in such a way that they remain in the asymptotic future of Σ and Eintein's equations are well-posed. The spatial slices Σ are therefore not "pierced" by singularities, they remain smooth [12,13]. An illustrative example is given by the usual Penrose diagram for a spherically symmetric collapse. It is possible to foliate the spacetime by spacelike hypersurfaces $\Sigma \simeq \mathbb{R}^3$, and they only intersect the curvature singularity for $t \to \infty$.

metric g_{ab}, that is solution of Einstein's equations. For each of them we can calculate the time-dependent quantity $F[g_{ab}](t) = \int_\Sigma d^3x\sqrt{-g}R_{abcd}{}^*R^{abcd}$. We can think of this as a quantity that keeps track of the chirality of the gravitational field as a function of time. As a pseudoscalar it flips sign under a reflection I of the metric (improper rotation) and remains invariant under a proper rotation R of the metric, namely $F[(R\circ I)g_{ab}] = -F[g_{ab}]$. If the metric of a binary system is invariant under a mirror transformation with respect to some coordinate plane, then one also has $F[(R\circ I)g_{ab}] = F[g_{ab}]$, and therefore $F[g_{ab}] = 0$ in these cases.

To give an illustrative example, consider a binary BH system in which the two spins are parallel to the orbital angular momentum, as in Fig. 1. These systems are nonprecessing, the orientation of the orbital angular momentum is constant (roughly speaking, the two BHs remain in a plane all the time). As a first approximation, we can assume that the gravitational field of the binary is equivalent to the gravitational fields of the two individual Kerr BHs (i.e., we ignore the nonlinearities associated to the mutual interaction). BHs are rigid compact objects, in the sense that tidal love numbers are zero or very small, so this approximation should work well. In this approximation, the entire spacetime geometry will be determined by the two masses and the two spins, because of the no-hair theorem. A simple analysis using symmetry arguments allows us to infer which binary systems can produce circularly polarized gravitational waves, i.e., if $F[g_{ab}](t) \neq 0$. First of all, take the system in a fixed instant of time, like in the upper figure of Fig. 1. Now perform a mirror transformation with respect to the coordinate plane normal to the separation between the two objects. The result is shown in the lower part of Fig. 1. Notice that the spins are pseudovectors, so one has to reverse sign under this transformation. Then, it is easy to see that we can find a continuous rotation in 3-space that returns the system back to the original configuration of masses and spins.

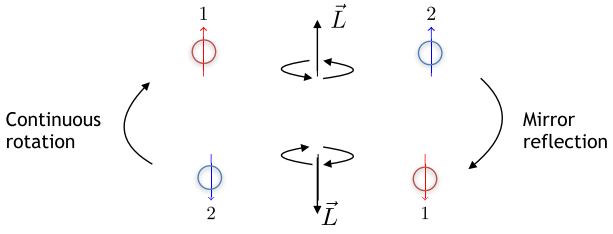

FIG. 1. Example of a binary BH system that is expected to yield a zero value of the Chern-Pontryagin (1). The picture represents one instant of time of a nonprecessing binary system with orbital angular momentum $\vec{L}$. The arrows 1 and 2 denote the individual spin vectors of each BH, and they keep aligned with $\vec{L}$ the whole evolution. The existence of a mirror symmetry in the metric produces $F[g_{ab}](t) = \int_\Sigma d^3x\sqrt{-g}R_{abcd}{}^*R^{abcd} = 0$ for any t. Numerical simulations confirm this theoretical prediction.

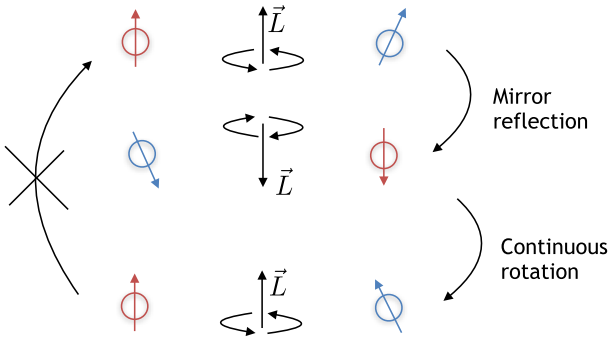

FIG. 2. Example of a binary BH system that is expected to yield a nonzero value of the Chern-Pontryagin (1). The picture represents one instant of time of the evolution of the binary, which has orbital angular momentum $\vec{L}$. The red and blue arrows denote the individual spin vectors of each BH, and are misaligned with $\vec{L}$. This produces the system to precess in time. The lack of a mirror symmetry in the metric can potentially yield $F[g_{ab}](t) = \int_\Sigma d^3x\sqrt{-g}R_{abcd}{}^*R^{abcd} \neq 0$ at each t. Numerical simulations confirm these theoretical expectations. In particular, the merger produces a flux of circularly polarized gravitational waves, as predicted in Eq. (2).

This simple example shows that nonprecessing binary BH systems have a mirror symmetry at any given time. Because $F[g_{ab}](t)$ is a pseudoscalar, it flips sign under mirror reflection. So at each instant of time we must necessarily have $F[g_{ab}] = 0$. In particular it also applies to nonspinning binary BHs, even in the unequal-mass case.

Most interestingly, the contrapositive of this statement tells us that for a spacetime to have a nonvanishing Chern-Pontryagin, it is required that the individual BH spins must be misaligned with the orbital-angular momentum. In other words, precessing binary BH systems can potentially lead to nonvanishing values of (1) and (2).[2] See Fig. 2 for an example of this. The mirror-symmetry arguments introduced in this section turn out to be really helpful in understanding the outcomes of numerical simulations.

III. NUMERICAL RESULTS FOR PRECESSING BHs

In the previous section we argued that precessing binary BH systems are the relevant configurations to explore the quantum effect of Eq. (1). In this section we confirm these theoretical expectations and extract the dependence of this quantity with the parameters of the binary.

To achieve this we perform numerical simulations using the $3+1$ numerical relativity code Einstein Toolkit [14,15], and the `McLachlan` thorn [16,17] for the spacetime evolution. We solve Einstein's equations for head-on, eccentric, and quasicircular BBH mergers, taking the

[2]Not all precessing BH system will lead to a nonzero effect as we will see in the next section.

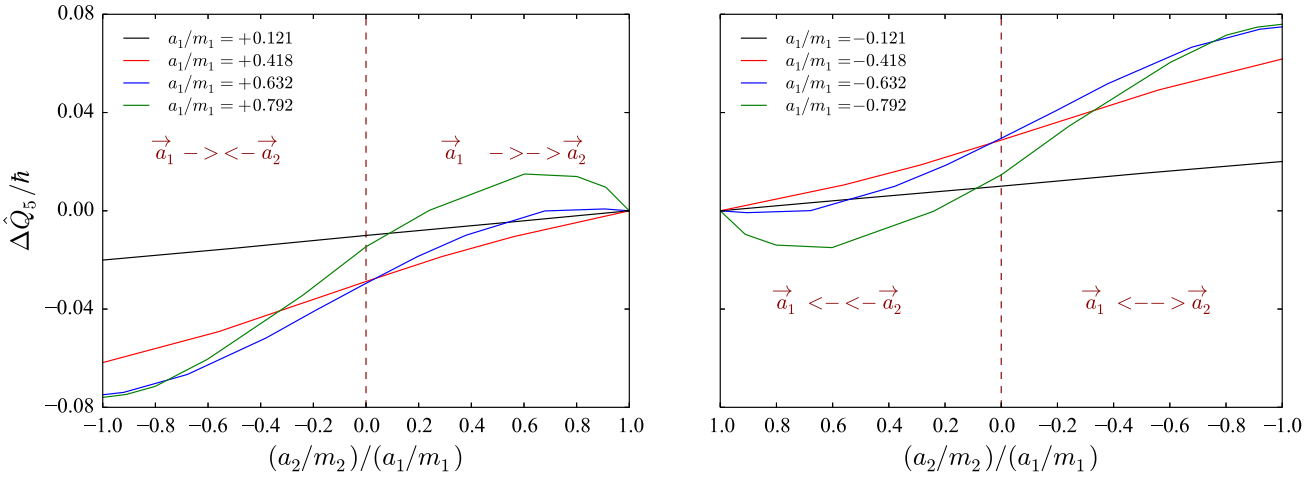

FIG. 3. Value of $\Delta\hat{Q}_5/\hbar$ calculated from (3) in head-on collisions as a function of the spin ratio a_2/a_1 for four different fixed values of a_1. As a_2 evolves from negative to positive values and viceversa, the binary system transitions between two relative spin orientations, indicated in each figure with two vectors on the real line. Notice how $\Delta\hat{Q}_5/\hbar$ flips sign when switching between the two figures, as expected from the mirror transformation underlying the figures.

component masses and initial linear momentum from [18]. To compute Eq. (1) we notice that

$$\Delta\hat{Q}_5 = -\frac{\hbar}{6\pi^2}\int_{t_1}^{t_2} dt\alpha \int_{\Sigma_t} d\Sigma_t \sqrt{h} E_{ij} B^{ij}, \tag{3}$$

where Σ_t is a spacelike hypersurface in our $3+1$ spacetime foliation, α is the lapse function, h_{ij} is the induced metric, and E_{ij}, B_{ij} are the electric and magnetic components of the Weyl tensor on Σ_t. We compute this by modifying the `Antenna` thorn [19,20] and the initial data are obtained using the `TwoPunctures` thorn [21]. As we will see later, the result of (3) will be dominated by the merger stage, so the specific choice of initial momenta and initial radial separation of the two black holes will not play a significative role. Our initial numerical grid is a superposition of two individual grids centered at the initial positions of the BHs. We make use of the `PunctureTracker` thorn, that tracks the location of each BH puncture during the evolution. Each individual grid has nine refinement levels with $\{(320, 160, 80, 40, 20, 5, 2.5, 1.25, 0.625), (4, 2, 1, 0.5, 0.25, 0.125, 0.0625, 0.03125, 0.015625)\}$. The first set of numbers indicates the size of the spatial domain of each level and the second set indicates the resolution. No symmetries are imposed on the numerical grids, therefore we have $x_{\min} = y_{\min} = z_{\min} = -320$ and $x_{\max} = y_{\max} = z_{\max} = 320$. We also use the Carpet adaptative mesh refinement for the Cactus framework [22] within the Einstein Toolkit infrastructure.

A. Head-on collisions

Head-on collisions provide the simplest setting to study the dependence of the Chern-Pontryagin with the spins in a binary system. In contrast to orbital mergers, the relative spin configuration remains roughly constant during the entire evolution, so that it is relatively easy to understand and interpret correctly the numerical results in terms of the framework described in Sec. II. The numerical exploration of head-on collisions can be particularly useful if we let the two individual BH spins be aligned with the velocity axis,

TABLE I. Value of the Chern-Pontryagin $\Delta\hat{Q}_5/\hbar$ computed from Eq. (3) using numerical-relativity simulations of binary BH mergers of equal mass and spin magnitude with orbital evolution. The S configurations correspond to binary systems where the initial BH spins have two nonvanishing cartesian components (of the same magnitude) in our coordinate system, as indicated in the second column, while the X configurations are binary BHs where the initial spins are aligned in the x direction. The spin orientations vary cyclically during the entire evolution. Roughly, they return to the same relative orientation after one orbital period. The results for $\Delta\hat{Q}_5/\hbar$ confirm the theoretical predictions described in Sec. II using symmetry arguments. In particular, those binary BHs with a configuration of spins with mirror symmetry produce a zero value of $\Delta\hat{Q}_5/\hbar$ (compatible with numerical inacuracies, see footnote 3).

Configuration	Initial spin orientation (x, y, z)	$\lvert a_i/m_i\rvert$	Total ADM mass	$\Delta\hat{Q}_5/\hbar$
S1	$(\leftarrow, 0, \uparrow), (\rightarrow, 0, \uparrow)$	0.312	1.03	0.040
S2	$(\leftarrow, 0, \uparrow), (\rightarrow, 0, \uparrow)$	0.520	1.12	−0.039
S3	$(\leftarrow, 0, \uparrow), (\rightarrow, 0, \uparrow)$	0.630	1.22	0.064
S4	$(\rightarrow, 0, \uparrow), (\rightarrow, 0, \uparrow)$	0.520	1.12	1.09×10^{-09}
S5	$(0, 0, \uparrow), (0, 0, \uparrow)$	0.630	1.22	3.42×10^{-11}
X1	$(\leftarrow, 0, 0), (\rightarrow, 0, 0)$	0.312	1.03	−0.051
X2	$(\leftarrow, 0, 0), (\rightarrow, 0, 0)$	0.520	1.12	0.105
X3	$(\leftarrow, 0, 0), (\rightarrow, 0, 0)$	0.630	1.22	0.086
X4	$(\rightarrow, 0, 0), (\rightarrow, 0, 0)$	0.630	1.22	1.15×10^{-09}

say in the x direction of our cartesian coordinate system, as $(\rightarrow,0,0),(\leftarrow,0,0)$ and $(\leftarrow,0,0),(\rightarrow,0,0)$. These two spin configurations are related by a mirror transformation, and both are expected to make (1) different from zero using the symmetry arguments of Sec. II.

To explore the impact of the spin magnitude on (1), we evolve a series of head-on collisions with these two spin configurations, fixing the spin magnitude of one of the BHs, a_1/m_1, and varying the other one in the range $a_2/m_2 \in (-a_1/m_1, a_1/m_1)$. The initial separation of the two BHs is not expected to play any important role in this problem so in all cases we fix $D = 11$ in code units. The results of four representative cases are summarized in Fig. 2, where we plot the values of the Chern-Pontryagin from Eq. (3) as a function of the ratio $(a_2/m_2)/(a_1/m_1)$ for four values of a_1/m_1. We conclude that the Chern-Pontryagin (3) reaches its maximum (in absolute value) when the two BHs have spins with equal magnitudes but opposite direction, while the $a_1 = a_2$ (with $m_1 = m_2$) configuration gives a zero contribution. In addition, the right panel of Fig. 2 shows that flipping the sign of a_1 only results in an overall change of sign in the Chern-Pontryagin, keeping the same magnitude. All these results confirm the validity of the analysis of mirror symmetry described in Sec. II above. It is worth noticing that even in the collision of a Kerr and of a Schwarzschild BHs, the resulting effect is nonzero (see Fig. 3).

B. Orbital mergers

While head-on collisions are useful to easily identify the role of the relative spin configurations on the Chern-Pontryagin, as well as its connection to the lack of mirror symmetry in the problem, it is also interesting to study the more astrophysically relevant case of orbital binary BHs to take into account the contribution of the inspiral phase. As we will detail shortly, the main new feature in this case is the presence of oscillations in the gravitational chirality during the evolution.

To explore this problem we perform nine equal-mass and equal-spin magnitude binary Kerr BH mergers in eccentric orbits. As before, we set the initial separation at $D = 11$,

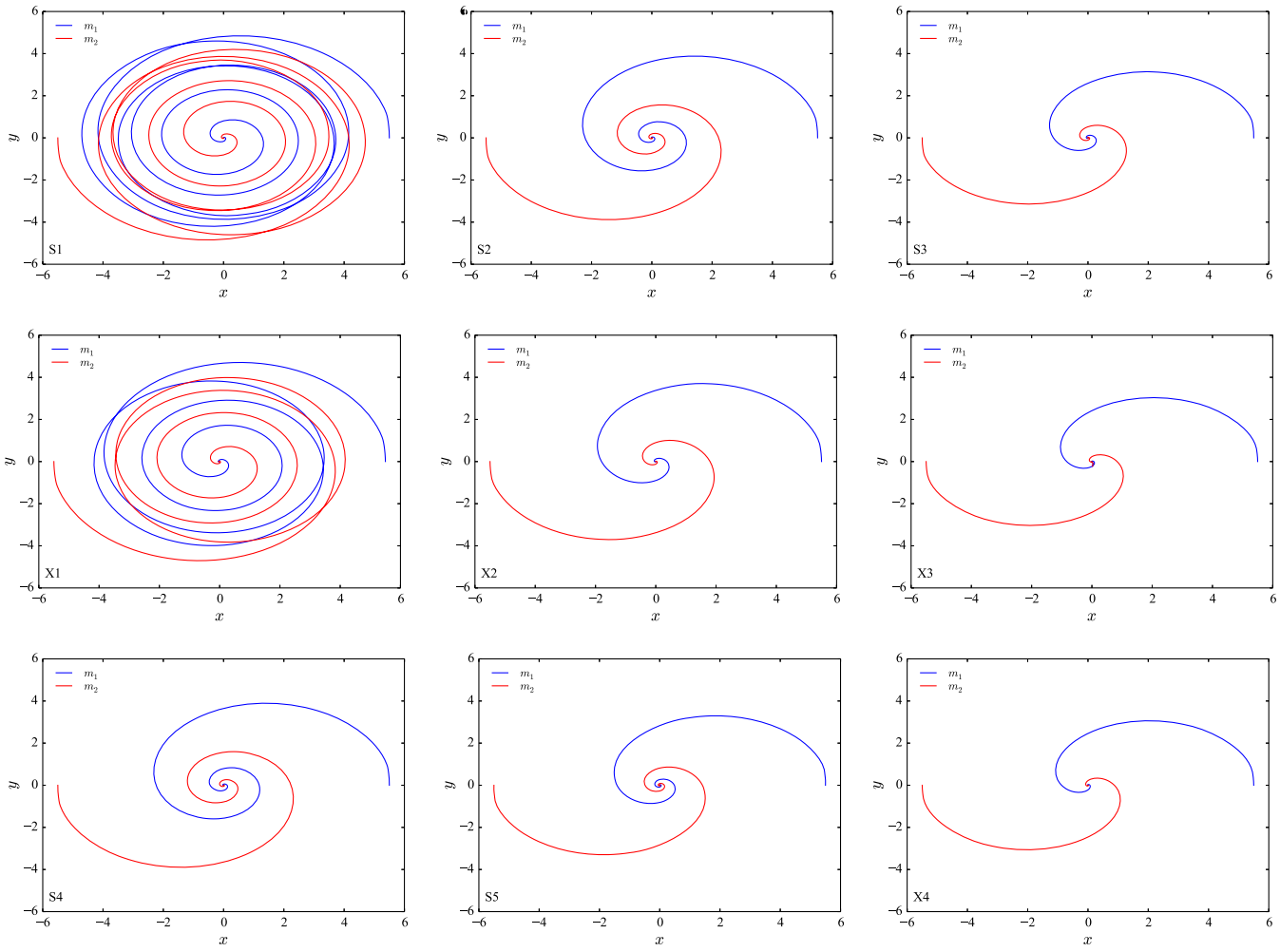

FIG. 4. Trajectories of the BHs projected on the equatorial xy ($z = 0$) plane for the different configurations described in Table I.

the initial momentum of the BHs to $|P_x| = 0.000728$ and $|P_y| = 0.0903$, and we vary their spin and mass. The details of each binary configuration can be found in Table I. As a result of varying both spin and mass without changing the initial separation and initial linear momentum, the orbital dynamics are drastically modified and we obtain different eccentric motions for the binary. This is shown in Fig. 4 where we plot the trajectories of the BHs in the equatorial plane ($z = 0$).

We have considered two main setups; in the first one, the spins are tilted 45 degrees with respect to the orbital plane and 90 degrees with respect to each other, $(\leftarrow, 0, \uparrow)$, $(\rightarrow, 0, \uparrow)$ (configurations S1, S2, S3); while in the other the spins have only a x-component and are anti-aligned, $(\leftarrow, 0, 0), (\rightarrow, 0, 0)$, as in the head-on case (configurations X1, X2, X3). Three additional cases are considered for completeness: a binary with aligned spins but tilted 45 degrees with respect to the orbital plane $(\rightarrow, 0, \uparrow)$, $(\rightarrow, 0, \uparrow)$ (configuration S4); a binary with both spins aligned with the orbital angular momentum $(0, 0, \uparrow)$, $(0, 0, \uparrow)$ (configuration S5); and a binary with aligned spins in the x direction $(\rightarrow, 0, 0), (\rightarrow, 0, 0)$ (configuration X4).

Most of the configurations studied here precess because the orientation of the spins have been chosen such that they are not aligned with the orbital angular momentum. The effect of precession is shown in Fig. 5 where we plot the trajectories of the BHs in the xz plane ($y = 0$). In general, both BHs start at $z = 0$ but move in the z plane. The only exception is the S5 configuration which consists of two aligned Kerr BHs with the orbital plane (bottom row, middle panel of Figs. 4 and 5). Despite this, not all precessing evolutions give a nonzero value of the Chern-Pontryagin. For instance, configurations S4 and X4 have the BH spins aligned with each other, but not aligned with the orbital angular momentum. In these cases, we also observe precession, which translates to non-negligible motion in the z plane (bottom row of Fig. 5). However,

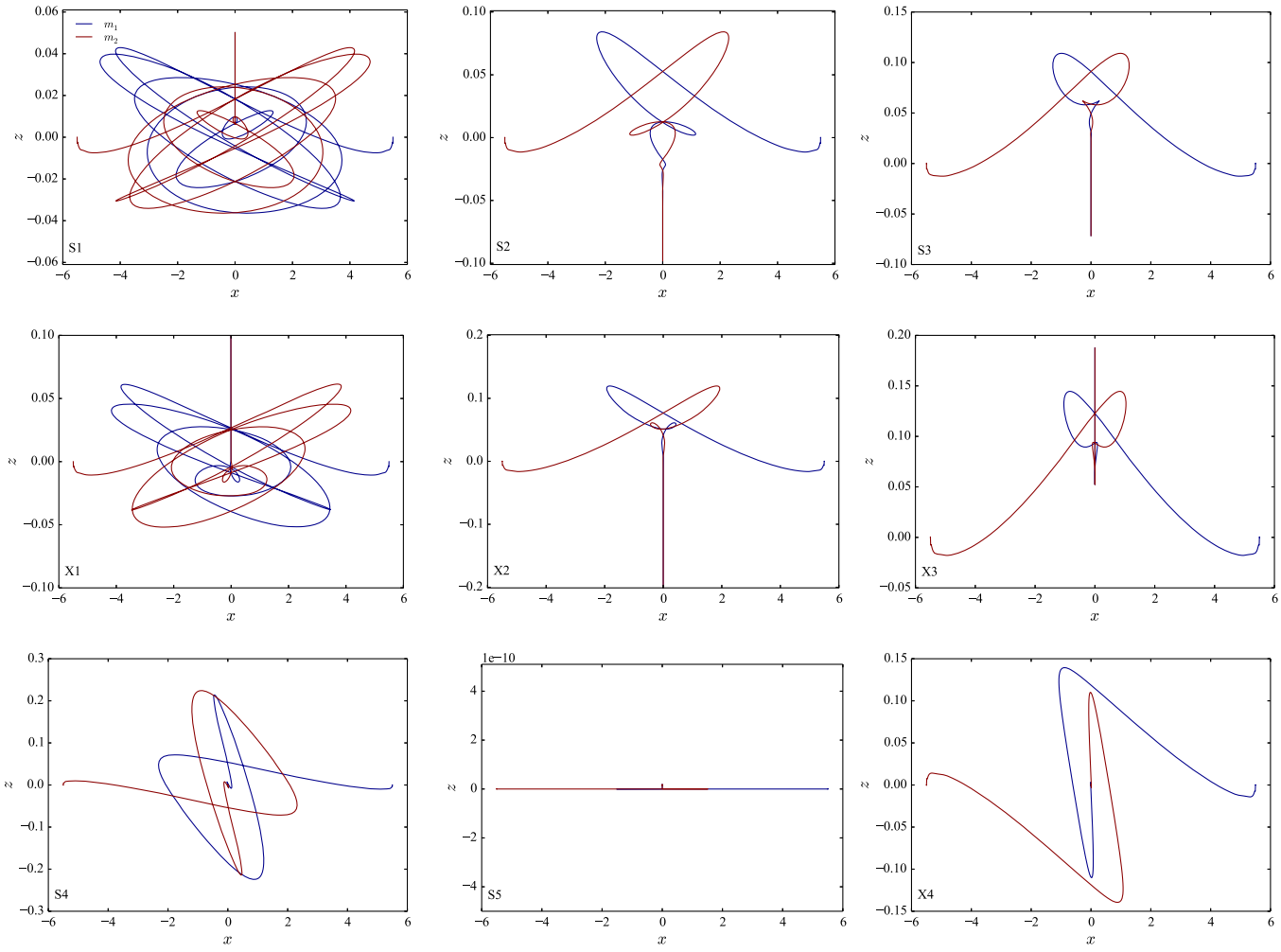

FIG. 5. Trajectories of the BHs projected on the xz plane (with $y = 0$) for the different configurations described in Table I. The existence of precession in the evolution is manifest in most cases. Configurations S1, S2, S3, X1, X2, and X3 give a nonzero contribution to the Chern-Porntryagin and also display a kick after the merger.

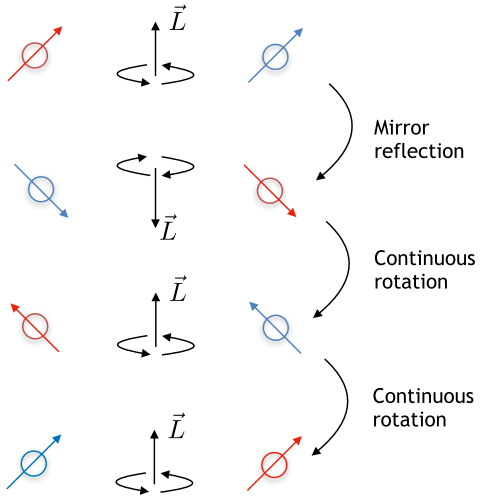

FIG. 6. Binary BH system with orbital evolution that may or may not yield a nonzero value of the Chern-Pontryagin (1). The picture represents one instant of time during the inspiral. The colors serve to distinguish the two BHs (each one with their own mass and spin magnitude). If the two BHs have the same masses and spins, then the system has a mirror symmetry which produces $F[g_{ab}](t) = \int_\Sigma d^3x\sqrt{-g}R_{abcd}{}^*R^{abcd} = 0$ at the time considered. Numerical simulations confirm this theoretical prediction. However, if the two BHs are distinguishable, there is no mirror symmetry and $F[g_{ab}](t) \neq 0$.

their contribution to the Chern-Pontryagin is compatible with zero[3] (see Table I). This could have been anticipated using arguments of mirror symmetry (see Fig. 6). It should be noted though that the Chern-Pontryagin vanishes only because we are considering equal-mass equal-spin BHs in this problem. If the mass or spin magnitude were different, we would have a nonzero effect.

From all these observations we can conclude that if $\Delta\hat{Q}_5/\hbar \neq 0$ then the system is necessarily precessing, but the converse is not necessarily true. On the other hand, the configurations with misaligned spins move along the z-axis and suffer a gravitational recoil or kick after the merger [23,24] as seen in Fig. 5. These configurations correspond precisely to the binaries that have a nonvanishing Chern-Pontryagin and would produce a flux of circularly polarized photons. Therefore, we find that there seems to be a connection between a nonzero Chern-Pontryagin, precession, and kicks. Our results suggest that all configurations with a nonvanishing $\Delta\hat{Q}_5/\hbar$ precess and are prone to kicks. However, the opposite is not necessarily true. Note that not all precessing systems give a nonzero contribution or suffer a kick, for instance the X4 configuration.

Since the Chern-Pontraygin (3) can be written as the time integral of a quantity that only depends on the geometry of the spatial slices in our $3+1$ spacetime decomposition, it is interesting to see explicitly the evolution in time of the geometrical quantity

$$\dot{Q}_5(t) = \int_{\Sigma_t} d\Sigma_t \sqrt{-g} E_{ij} B^{ij}. \tag{4}$$

Notice that, in contrast to (1), this magnitude does depend on the total mass M_* of the binary, as $1/M_*$. The integration in time cancels this dependence though.

Figure 7 shows the time evolution of this quantity for the nine simulations. For instance, in the upper-left panel, which corresponds to configurations S1 and X1 in Table I, we see that $\dot{Q}_5(t)$ oscillates around zero. This is in fact the general result in all orbiting cases where the Chern-Pontryagin is not zero. To understand correctly this behaviour we have to recall the analysis of symmetries of Sec. II. Suppose a quasicircular binary system. The relative orientation of the two BH spins evolve cyclically in time during the inspiral. In particular, given a particular spin configuration at some instant of time t_0, with value $\dot{Q}_5(t_0)$, after half orbital period T the new configuration of BH spins gets exactly the mirror-reflected version of the system at time t_0. If additionally the separation distance remains roughly constant during this half-period, we can expect $\dot{Q}_5(t_0 + T/2) \approx -\dot{Q}_5(t_0)$. Then, after one full orbital period, the relative spin configuration returns to the same state, and we can again expect $\dot{Q}_5(t_0 + T) \approx \dot{Q}_5(t_0)$. The smaller the separation distance between the BHs, the greater this effect will be (because gravity gets more extreme). Therefore, the oscillations are expected to increase adiabatically during the whole inspiral, until BHs merge and we observe a sharp rise corresponding to the maximum peak in the plots. After the merger and formation of the final BH, the value goes to zero very quickly, as expected for a stationary Kerr BH. All these expectations are clearly manifested in Fig. 8, which shows in more detail the time evolution of $\dot{Q}_5(t)$ together with the evolution of the x and z coordinates of both BHs. The maxima and minima of $\dot{Q}_5(t)$ are obtained approximately when the BHs are again located on the x axis with $y = 0$ (solid black and dashed red lines). This is due to the initial setup, in which the initial spins are positioned in an extremal configuration for the Chern-Pontryagin $(\leftarrow, 0, 0)$, $(\rightarrow, 0, 0)$. Due to the orbital motion, when the black holes cross the y-axis (with $x = 0$) the configuration becomes minimal [$\dot{Q}_5(t)$ vanishes] due to mirror symmetry. However, when they reach half an orbit and the black holes are back on the x-axis (with $y = 0$), we find an extremal spin configuration but with opposite sign $(\rightarrow, 0, 0)$, $(\leftarrow, 0, 0)$. Finally, when the orbit is complete and again the black holes are located on the x-axis, we have the extremal configuration of the beginning

[3]Note that a zero value cannot be strictly attained due to the numerical truncation errors. The nonzero values obtained for the S4, S5, and X4 configurations are the result of numerical accuracy, which, for the same resolution, may vary depending on the binary orbital dynamics and the precession they undergo. Our convergence study (see the Appendix) shows that such values do converge to zero as the resolution increases.

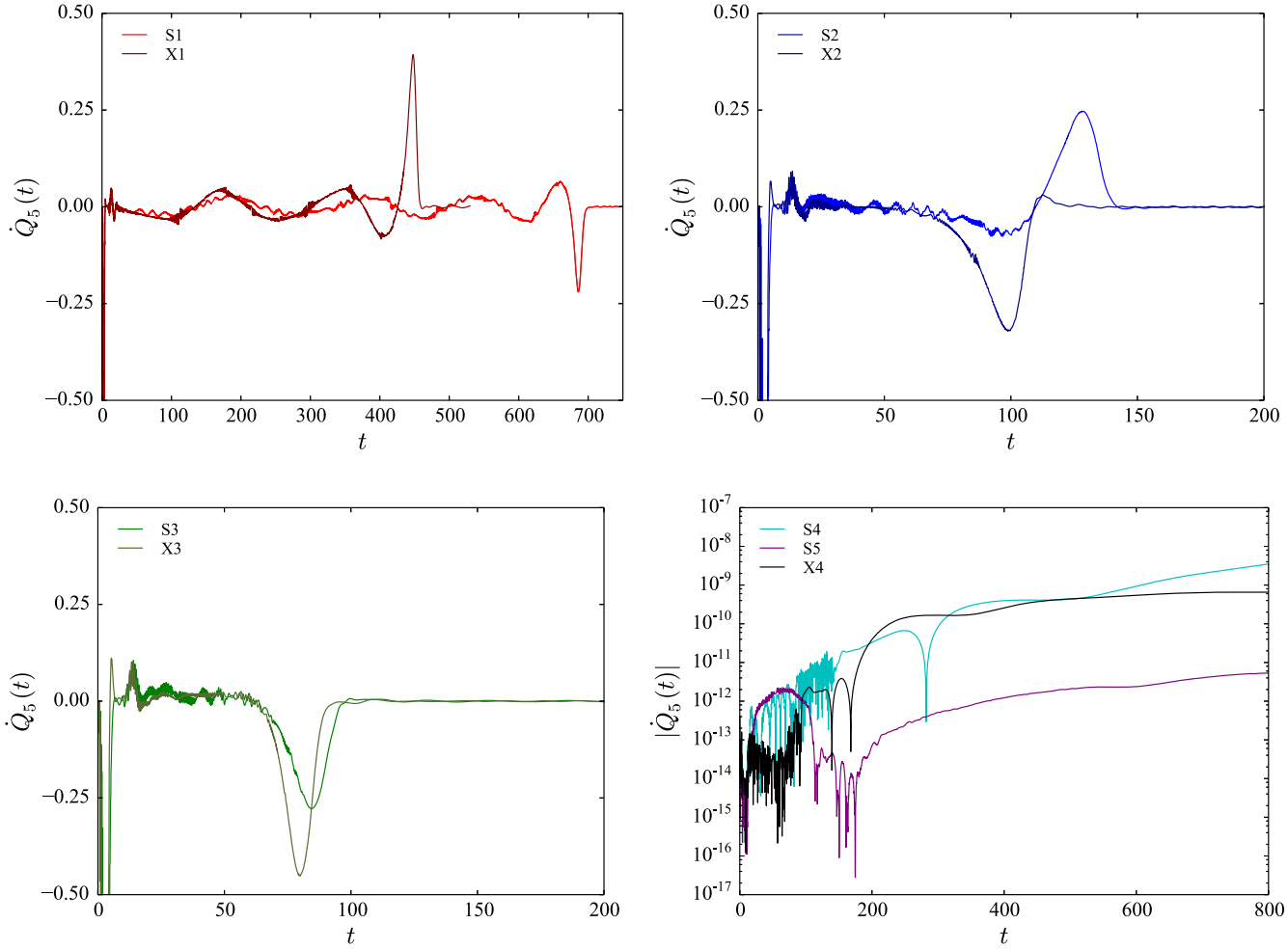

FIG. 7. Time evolution of $\dot{Q}_5$ computed from (4) for the nine binary BH configurations described in Table I. In cases when $\Delta\hat{Q}_5/\hbar \neq 0$ (top left and right panels, bottom left panel), $\dot{Q}_5(t)$ oscillates in time around zero during the inspiral phase all the way up to the merger. This periodicity in $\dot{Q}_5(t)$ is a manifestation of the cyclic evolution of the relative spin configuration of the two BHs during inspiral (see main text for details). The largest positive or negative peaks correspond to the time of merger, after which $\dot{Q}_5(t)$ drops down to zero, as expected for a stationary Kerr BH.

(although the distance between the objects has been slightly reduced). At similar times, their position in the z-axis $|z_i|$ (solid dark blue and orange dotted lines) also becomes maximum.

The contribution of the inspiral to the Chern-Pontryagin $\Delta\hat{Q}_5/\hbar$ is small since, as commented above, the orbital motion changes the spin configuration cyclically and leads to consecutive positive and negative peaks in $\dot{Q}_5(t)$ that almost cancel each other out after integrating in time. The most important contributions to $\Delta\hat{Q}_5/\hbar$ come from the last orbit and the merger. It is during the merger that we get the largest positive or negative peaks shown in the plots of Fig. 7. In quasicircular binaries (see upper left panel of Fig. 7) there is also a previous large amplitude peak with opposite sign that can cancel an important part of the final maximum peak when computing the total time-integrated quantity. However, as the orbits become more and more eccentric (upper right and lower left panels of Fig. 7), and in particular for head-on collisions, there is only one final peak. Therefore, it is for highly eccentric collisions that the maximum net effect for $\Delta\hat{Q}_5/\hbar$ could be expected. On the other hand, the bottom-right panel of Fig. 7 displays the time evolution of $\dot{Q}_5$ in cases when the two BH spins are aligned (configurations S4, S5, X4), and for which the binary BH retains some mirror symmetry. In these cases not only the Chern-Pontryagin $\Delta\hat{Q}_5/\hbar$ vanishes, as shown in Table I, but $\dot{Q}_5(t)$ is zero (within the numerical error) at all times, in excellent agreement with our theoretical interpretation in Sec. II.

Finally, Fig. 9 shows how the Chern-Pontryagin (3) changes as a function of the spin parameter for different collisions and spin configurations. The comparison is not entirely accurate, since in the orbital case the trajectories are different for each binary and the final result may vary depending on the dynamics, but it serves as an illustrative estimate of the behaviour of the Chern-Pontryagin in these

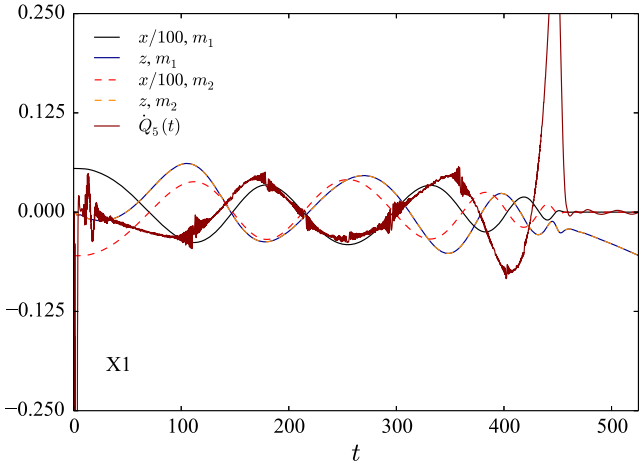

FIG. 8. Time evolution of $\dot{Q}_5$ computed from (4) for configuration X1 of Table I (solid dark red line). The x (divided by 100) and z coordinates of each BH are also shown as a function of time. Notice the high correlation between the value of $\dot{Q}_5$ and the position of the BHs along the orbit. This supports the theoretical interpretation described in the main text.

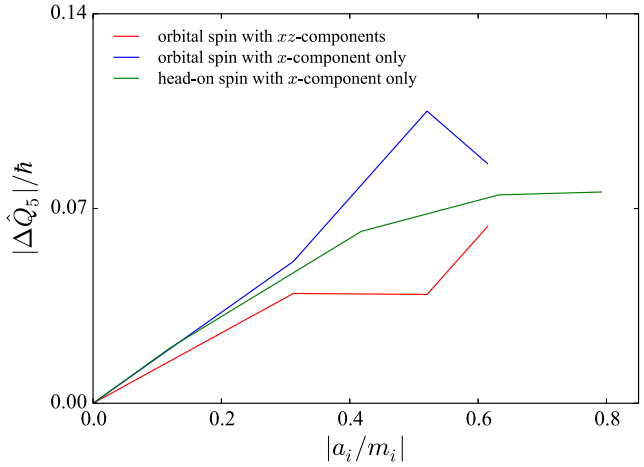

FIG. 9. Absolute value of $\Delta\hat{Q}_5/\hbar$ computed from (3) as function of the spin parameter a_i/m_i for equal-mass and equal-spin orbital binary BH mergers with different spin inclinations with respect to the orbital plane; 45 degrees (red line) and 90 degrees (blue line). The green line corresponds to equal-mass and equal-spin head-on collisions with spins inclined 90 degrees.

scenarios. The conclusion is that (3) is maximized when the spins are as misaligned as possible with respect to each other and with respect to the orbital angular momentum. As expected, the more the mirror symmetry is broken in the binary, the higher the value of (3) is.

IV. CONCLUSIONS AND FURTHER APPLICATIONS

Motivated by quantum considerations, in this work we carried out a throughout study of the Chern-Pontryagin curvature scalar (1) to figure out what are the key elements of binary BH systems that may trigger the spontaneous creation of photons with net helicity through quantum vacuum fluctuations. To this end we have performed a series of numerical simulations of head-one collisions and eccentric orbital mergers, with specific configurations of masses and spins motivated on arguments of mirror symmetry. Our findings indicate that orbital precession of the two BHs, or equivalently the misalignment of the two spins with the orbital angular momentum, can produce the required helicity violation.

As remarked above, we solved the dynamical evolution of these BHs with numerical relativity simulations. However, the use of symmetry arguments has proven to be extremely efficient to understand correctly the numerical results. Our theoretical expectations have been validated one by one in the simulations. Given the highly nonlinear nature of Einstein's equations and of the systems involved, it is remarkable that one can predict the outcomes of a quadratic curvature integral over the whole spacetime using simple arguments on mirror symmetry. In fact, the use of symmetry breaking may be helpful to gain further insights on the dynamics of binary BHs. More precisely, the exploitation of mirror symmetry in Sec. II above allowed us to predict that a necessary condition for (1) and (2) to be nonzero is that the binary is precessing. Currently, the identification of precessing binary BHs among all the observed events in LIGO-Virgo interferometers is an open problem and, although many events are expected to precess, there is only partial evidence of this in one single event GW200129 [25–27] (and in fact it is not free of controversy [28]). Precession is expected to produce a small modulation on the gravitational waveforms, but detecting this requires more precision and searches that include this effect [29–31]. Alternatively, symmetry arguments guarantee that if (2) is not zero, then the binary is necessarily precessing. In other words, the inference of net, non-negligible gravitational-wave circular polarization from LIGO-Virgo detections can be used to identify precessing systems.[4] This independent observable may pave the way for identifying precession systematically. We plan to explore this possibility in future works [32].

Another interesting feature is that there seems to be a correlation between precessing binaries with non-zero Chern-Pontryagin and kicks due to gravitational-wave emission. This is somewhat expected; on the one hand,

[4]Notice that Eq. (2) represents the *net*, circularly polarized flux of gravitational waves emitted by a binary, integrated among *all* directions on the sphere. While nonprecessing binaries can generate a gravitational wave mode (ℓ, m) with circular polarization, i.e., $|h_+^{\ell m}(\omega) - ih_\times^{\ell m}(\omega)|^2 - |h_+^{\ell m}(\omega) + ih_\times^{\ell m}(\omega)|^2 \neq 0$, the mirror-symmetric mode $(\ell, -m)$ cancels this contribution upon summation in (2). An unbalance is only obtained when the binary black hole is precessing, i.e., when the mirror symmetry is broken.

kicks can be measured from the gravitational waves emitted by the system [30] and are expected to be originated from an asymmetry in the direction of the gravitational emission, that pushes the BH out of the orbital plane due the gravitational waves carrying linear momentum [33]. On the other hand, if the positive and negative modes m of the spin-weighted spherical harmonics do not compensate each other, this is a indication of mirror asymmetry and therefore the Chern-Pontryagin [10] is different from zero. It may be possible that in some cases both asymmetries are connected [34,35].

From a quantitative point of view, the results obtained for helicity violation in photons are rather small, the order of magnitude is similar to the Hawking radiation effect, roughly one photon of difference between the right-handed and left-handed fluxes for each merger. This is not really surprising, and taken at face value, it seems very unlikely that one may be able to observe this quantum effect directly for one single event. However, it should be noted that small numbers can seed macroscopic effects through classical amplification mechanisms. Besides, in large enough numbers the quantum effect may lead to significant implications. More precisely, if the formation channels of binary black holes in astrophysics favour "right-handed" spin configurations over "left-handed," or vice versa, this may produce an accumulated effect in the Universe. This is out of the scope of the present paper, our plan is to investigate this in more detail in the future [32].

ACKNOWLEDGMENTS

We thank José A. Font, Ivan Agullo, and José Navarro-Salas for useful discussions, and specially Juan Calderón Bustillo for discussions regarding the current experimental evidence of precession in binary mergers. N. S. G. is supported by the Spanish Ministerio de Universidades, through a María Zambrano grant (ZA21-031) with Reference No. UP2021-044, funded within the European Union-Next Generation EU. A. D. R. is supported through a M. Zambrano grant (ZA21-048) with Reference No. UP2021-044 from the Spanish Ministerio de Universidades, funded within the European Union-Next Generation EU. This work has further been supported by the European Horizon Europe staff exchange (SE) programme HORIZON-MSCA-2021-SE-01 Grant No. NewFunFiCO-101086251. This work is also supported by the Spanish Agencia Estatal de Investigación (Grant No. PID2021-125485NB-C21). N. S. G. thankfully acknowledges the computer resources at Tirant and the technical support provided by UV (RES-FI-2022-3-0006).

APPENDIX: CODE ASSESSMENT

We briefly comment here on the convergence analysis we carried out to assess the quality of our simulations. To perform the binary black hole evolutions we have employed the freely-available Einstein Toolkit code. Further convergence tests can be found in [14,15]. In Fig. 10 we plot the volume integral of the Chern-Pontryagin as a function of time $\dot{Q}_5(t)$ computed for configurations S4 and X3, which correspond to precessing systems with aligned and nonaligned spins respectively, using three different resolutions with $dx = dy = dz = \{0.03125, 0.01953125, 0.015625\}$ in the finest level. In the bottom panel of Fig. 10 we show that the Chern-Pontryagin converges to zero at the expected fourth-order rate for the S4 configuration, confirming our symmetry analysis.

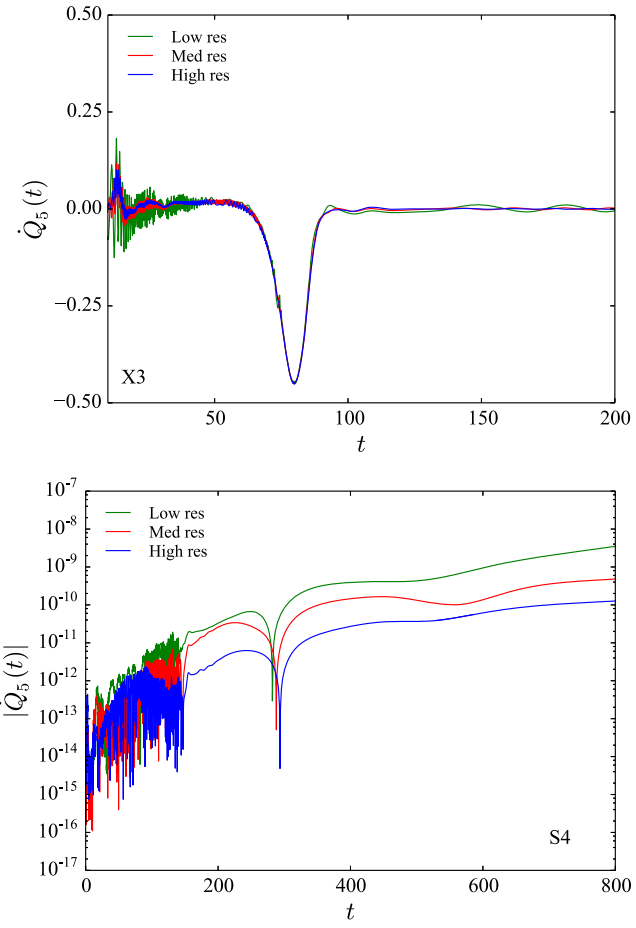

FIG. 10. Time evolution of $\dot{Q}_5$ for configurations X3 (top panel) and S4 (bottom panel) using three different resolutions with $dx = dy = dz = \{0.03125, 0.01953125, 0.015625\}$ in the finest level.

[1] N. D. Birrell and P. C. W. Davies, *Quantum Fields in Curved Space*, Cambridge Monographs on Mathematical Physics (Cambridge University Press, Cambridge, England, 1982).

[2] L. Parker and D. Toms, *Quantum Field Theory in Curved Spacetime: Quantized Fields and Gravity*, Cambridge Monographs on Mathematical Physics (Cambridge University Press, Cambridge, England, 2009).

[3] L. Parker, Particle Creation in Expanding Universes, Phys. Rev. Lett. **21**, 562 (1968).

[4] S. W. Hawking, Particle creation by black holes, Commun. Math. Phys. **43**, 199 (1975).

[5] D. N. Page, Particle emission rates from a black hole. II. Massless particles from a rotating hole, Phys. Rev. D **14**, 3260 (1976).

[6] I. Agullo, A. del Rio, and J. Navarro-Salas, Electromagnetic Duality Anomaly in Curved Spacetimes, Phys. Rev. Lett. **118**, 111301 (2017).

[7] I. Agullo, A. del Rio, and J. Navarro-Salas, Gravity and handedness of photons, Int. J. Mod. Phys. D **26**, 1742001 (2017).

[8] I. Agullo, A. del Rio, and J. Navarro-Salas, Classical and quantum aspects of electric-magnetic duality rotations in curved spacetimes, Phys. Rev. D **98**, 125001 (2018).

[9] I. Agulló, A. del Río, and J. Navarro-Salas, On the Electric-magnetic duality symmetry: Quantum anomaly, optical helicity, and particle creation, Symmetry **10**, 763 (2018).

[10] A. del Rio, N. Sanchis-Gual, V. Mewes, I. Agullo, J. A. Font, and J. Navarro-Salas, Spontaneous Creation of Circularly Polarized Photons in Chiral Astrophysical Systems, Phys. Rev. Lett. **124**, 211301 (2020).

[11] A. del Rio, Chiral anomalies induced by gravitational waves, Phys. Rev. D **104**, 065012 (2021).

[12] M. Hannam, S. Husa, D. Pollney, B. Brügmann, and N. O. Murchadha, Geometry and Regularity of Moving Punctures, Phys. Rev. Lett. **99**, 241102 (2007).

[13] M. Alcubierre, *Introduction to 3+1 Numerical Relativity* (OUP, Oxford, 2008), Vol. 140.

[14] Einstein Toolkit, Open software for relativistic astrophysics, http://einsteintoolkit.org (2012).

[15] F. Löffler, J. Faber, E. Bentivegna, T. Bode, P. Diener, R. Haas, I. Hinder, B. C. Mundim, C. D. Ott, E. Schnetter *et al.*, The Einstein Toolkit: A community computational infrastructure for relativistic astrophysics, Classical Quantum Gravity **29**, 115001 (2012).

[16] D. Brown, P. Diener, O. Sarbach, E. Schnetter, and M. Tiglio, Turduckening black holes: An analytical and computational study, Phys. Rev. D **79**, 044023 (2009).

[17] C. Reisswig, C. D. Ott, U. Sperhake, and E. Schnetter, Gravitational wave extraction in simulations of rotating stellar core collapse, Phys. Rev. D **83**, 064008 (2011).

[18] W. Tichy and B. Brügmann, Quasiequilibrium binary black hole sequences for puncture data derived from helical killing vector conditions, Phys. Rev. D **69**, 024006 (2004).

[19] J. Baker, M. Campanelli, and C. O. Lousto, The Lazarus project: A pragmatic approach to binary black hole evolutions, Phys. Rev. D **65**, 044001 (2002).

[20] M. Campanelli, B. Kelly, and C. O. Lousto, The Lazarus project. II. Spacelike extraction with the quasi-Kinnersley tetrad, Phys. Rev. D **73**, 064005 (2006).

[21] M. Ansorg, B. Brügmann, and W. Tichy, Single-domain spectral method for black hole puncture data, Phys. Rev. D **70**, 064011 (2004).

[22] Carpet: Adaptive mesh refinement for the cactus framework, https://bitbucket.org/eschnett/carpet.git.

[23] J. A. Gonzalez, U. Sperhake, B. Bruegmann, M. Hannam, and S. Husa, Maximum Kick from Nonspinning Black-Hole Binary Inspiral, Phys. Rev. Lett. **98**, 091101 (2007).

[24] J. A. González, M. Hannam, U. Sperhake, B. Bruegmann, and S. Husa, Supermassive Recoil Velocities for Binary Black-Hole Mergers with Antialigned Spins, Phys. Rev. Lett. **98**, 231101 (2007).

[25] R. Abbott, T. Abbott, F. Acernese, K. Ackley, C. Adams, N. Adhikari, R. Adhikari, V. Adya, C. Affeldt, D. Agarwal *et al.*, GWTC-3: Compact binary coalescences observed by LIGO and Virgo during the second part of the third observing run, arXiv:2111.03606.

[26] V. Varma, S. Biscoveanu, T. Islam, F. H. Shaik, C.-J. Haster, M. Isi, W. M. Farr, S. E. Field, and S. Vitale, Evidence of Large Recoil Velocity from a Black Hole Merger Signal, Phys. Rev. Lett. **128**, 191102 (2022).

[27] M. Hannam, C. Hoy, J. E. Thompson, S. Fairhurst, V. Raymond, M. Colleoni, D. Davis, H. Estellés, C.-J. Haster, A. Helmling-Cornell *et al.*, General-relativistic precession in a black-hole binary, Nature (London) **610**, 652 (2022).

[28] E. Payne, S. Hourihane, J. Golomb, R. Udall, D. Davis, and K. Chatziioannou, Curious case of GW200129: Interplay between spin-precession inference and data-quality issues, Phys. Rev. D **106**, 104017 (2022).

[29] I. Harry, S. Privitera, A. Bohé, and A. Buonanno, Searching for gravitational waves from compact binaries with precessing spins, Phys. Rev. D **94**, 024012 (2016).

[30] J. C. Bustillo, P. Laguna, and D. Shoemaker, Detectability of gravitational waves from binary black holes: Impact of precession and higher modes, Phys. Rev. D **95**, 104038 (2017).

[31] K. Chandra, V. Gayathri, J. C. Bustillo, and A. Pai, Numerical relativity injection analysis of signals from generically spinning intermediate mass black hole binaries in Advanced LIGO data, Phys. Rev. D **102**, 044035 (2020).

[32] J. C. Bustillo, A. Del Rio, and N. Sanchis-Gual (to be published).

[33] W. Tichy and P. Marronetti, Binary black hole mergers: Large kicks for generic spin orientations, Phys. Rev. D **76**, 061502 (2007).

[34] J. Calderón Bustillo, J. A. Clark, P. Laguna, and D. Shoemaker, Tracking Black Hole Kicks from Gravitational-Wave Observations, Phys. Rev. Lett. **121**, 191102 (2018).

[35] J. C. Bustillo, S. H. Leong, and K. Chandra, GW190412: Measuring a black-hole recoil direction through higher-order gravitational-wave modes, arXiv:2211.03465.